A wavelet based method for electrical stimulation artifacts removal in electromyogram

Maxime Yochum, Stéphane Binczak

A wavelet based method for electrical stimulation artifacts removal in electromyogram

Maxime Yochum, Stéphane Binczak

Laboratoire LE2I UMR CNRS 6306, Universit de Bourgogne, 9 avenue Alain Savary, 21078 Dijon, France. (e-mail: stbinc@u-bourgogne.fr)

Abstract

A technique for artifact removal based on the continuous wavelet transform is presented. It uses common mother wavelets to find the temporal localization of stimulation artifacts on electromyogram signal recording during an electrical surface evoked contraction of a muscle. This method is applied with different kinds of stimulation pulse parameters including shape and duration changes. This method is used with standard stimulation pulse waveforms such as monophasic or biphasic ones. It can also be applied when the artifacts and M waves are in the same range of amplitude where threshold techniques are inefficient. Lastly, a method to determine which mother wavelet efficiently removed artifacts is proposed, results indicate the Haar wavelet performs best among fourteen tested wavelets.

Keywords: Artifact removal, Electromyogram , wavelet, M wave.

1. Introduction

The Electromyogram (EMG) captures the electrical response of the muscle over its contraction whether muscular contraction is voluntarily or electrically induced. During a myo-electrical stimulation (ES), EMG contains two major sources. The first one is the muscular electrical activity generated by the stimulated muscle due to the contractions of muscular fibers. Sometimes, EMG also records the electrical activities of adjacent muscles which can be recruited with the same electrical stimulation [1]. It is a useful signal to study physiological characteristics of muscles over a contraction, especially in case of muscular or neurological diseases [2, 3]. The second source is composed of electrical stimulation artifacts [4] which disturb the study of electrical muscular activities. In order to properly analyze the EMG signal, stimulation artifacts need to be removed [5, 6]. Several techniques are already used to attenuate the impact of artifacts on EMG signals. These techniques can be split in two categories which are hardware or computation processing.

Hardware:
These techniques are often implemented with respect to EMG electrodes and differential amplifier circuitry design. To cite some of them:

- Analog filtering methods are designed to remove high frequencies of EMG which contain artifacts. However, it is very difficult to filter artifacts without modifying M waves. For instance, an 8th order Chebyshev low pass filter with a 550 Hz cutoff frequency has been implemented by Solomonow et al. [7] to remove artifacts. However, these types of filters allow passage of low frequency artifacts and may also remove parts of M waves residing in the same frequency range of artifacts [8].

- Methods based on hardware amplifier gain utilized by Roskar and Roskar [9] set amplifier gains to obtain a unit gain during electrical stimulation pulses and a gain of 1000 elsewhere. However, a gain of 1000 insufficiently eliminates major artifacts [5] and lacks robustness to adapt to changes in electrical stimulation applied to magnitude or frequency.

- Blanking hardware methods consist of disconnecting (electrical isolation) EMG electrodes from the muscle during electrical stimulation. Generally, a triggering synchronization from the electrical stimulator is used [10–12]. The drawback of this technique is that the blanking window is fixed and can lead to residual artifacts if the blanking duration is too short or can lead to unintended removal of M waves when the blanking duration is too long.

- Other hardware methods can be mixed such as those implemented by Nikolic et al. [13] who use blanking and filtering at the same time.

Computation processing:
Some techniques are implemented in software with computation processing as a pre-processing of EMG signal. Here, we briefly discuss methods using recordings of the stimulation artifact signal in order to subtract it from the EMG. Three main techniques exist to record an estimation of the stimulation artifact signal: a stimulation below the muscular contraction threshold (stimulation that does not cause any muscle contraction), a record far away from the EMG electrodes placement [1] (a second EMG is collected away from the first one to acquire pure artifacts) and a dual pulse stimulation (a second stimulation pulse is done during the refractory period which does not create any evoked signal, only the stimulus artifact is recorded) [14]. These techniques may be unable to remove all artifacts and tend to degrade the signal to noise ratio (SNR). In addition, the recorded artifact must be very accurate for a better removal

process [15], which often requires supplementary hardware.
In methods based on threshold detection [16], stimulation artifacts are mostly higher than M wave amplitude by a factor of 2 or 3 [5]. This difference in magnitude is then used to distinguish between the artifact and the M wave parts. Nevertheless, it may not be suitable to specific stimulation for which the amplitude of M waves and artifacts are close.
Other mathematical methods can estimate stimulation artifacts, like curves fitting or artifact models, in order to remove them [17–19].

Possible drawbacks of the hardware technique is that it requires knowledge of when stimulations are sent to the muscle, which is the case for both amplifier gain and blanking methods. Therefore, those techniques cannot be used when electrical stimulators are not adapted. In addition, the operating window is fixed and lead to partial artifact interference. Regarding the filtering methods, they can easily be implemented in a software processing scheme without need of additional hardware circuitry. Filtering methods can also attenuate artifacts parts which merge with M waves. However, the use of filtering techniques do not guarantee artifacts are removed without modifying the M waves, which may cause a miscomputation of physiological muscle features [20]. The disadvantage of software methods using threshold techniques is the difficult determination of the threshold, especially when artifacts are in the same amplitude range of the M waves [16].

In this context, we propose a new method to remove stimulation artifacts from EMG during a rehabilitation process with an electrical stimulation by using a continuous wavelet transform (CWT) and a histogram representation. CWT is a useful tool for biomedical signal processing [21]. The aim is to find the time localization of both artifact and M waves in the CWT domain in order to erase artifacts. The threshold is automatically found to avoid aforementioned difficulties from manual selection uncertain manually choice. We show that even when the amplitudes of artifacts and M waves are equivalent, CWT domain analysis can provide a suitable separation between them. To present the removal method, the Haar mother wavelet is used. In order to check flexibility of our approach we test different but common stimulation pulse shapes, which are monophasic, biphasic and dual biphasic, and different stimulation pulse durations. Indeed, when the stimulation changes in its shape, the artifact and the M wave evolved [22] such that the presented artifact removal approach was not impaired with these modifications. Next, results obtained with a panel of other mother wavelets are displayed, leading to selection of the most promising decomposition. Lastly, two indexes were proposed showing that the Haar wavelet best distinguished artifacts and M waves apart.

2. Material and Method

2.1. data set recording

The material used for our experiments delivered the electrical stimulation and performed EMG signal acquisition in real time [23]. The electrical stimulator generated controlled current pulses and constant stimulation with a maximum of $\pm 100\ mA$ for a body impedance of 1.5 $K\Omega$ between the two stimulation electrodes, a frequency pulse train from 10 Hz to 100 Hz and a pulse duration from 0.5 ms to 2 ms for 5 different pulse shapes most common in the literature (monophasic, biphasic, dual biphasic, absorbed biphasic and N-let). The EMG amplifier recorded EMG from muscle during the stimulation with bipolar electrodes and a reference electrode. Instrumentation amplifiers used for the circuit included the INA128 from Texas Instruments with a 120 dB of Common Mode Rejection Ratio for a removal of common voltage from bipolar electrodes with a high input impedance (>1GΩ). The M waves extracted from the global EMG signal during evoked contractions were used to estimate the fatigue level of the muscle during the rehabilitation session [24]. The EMG signal was saved with a sample rate of 10 kHz. A dedicated software allowed management of stimulation parameters and analysis of muscular fatigue level following artifact pre-processing software among three methods: blanking, thresholding algorithm or the method proposed in this study.

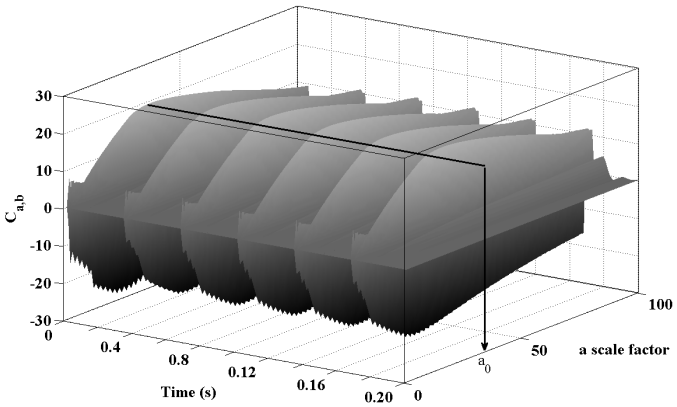

Figure 1: Example of continuous wavelet transform result with Haar mother wavelet from V_{EMG} signal plotted in Figure 2 a. scale factors go from 1 to 100. The a_0 scale factor corresponding with the maximum of $C_{a,b}$ is represented with the black arrow line.

All experiments were carried out on the right biceps muscle in an isometric position where the skeleton remained fixed. Subjects were placed in a Biodex pro 3 device [25] to be sure that the isometric position, carried on throughout the contraction, was maintained. The experiments were carried out on five subjects (mean 24 ±2 years) with bipolar (10 mm disk Ag/AgCl from Nessler) electrodes with liquid conductor gel. Electrodes were placed over the target muscle belly, parallel with the muscles fibers (tendon to tendon axis). Electrode placement was compliant with EMG processing standard [26]. Ten different kinds of stimulation were performed on each subject including variation in amplitude, frequency, pulse duration and form shape of the stimulation parameters. Each stimulation train was six seconds long. Our experiments provided a data base of fifty samples of EMG signals.

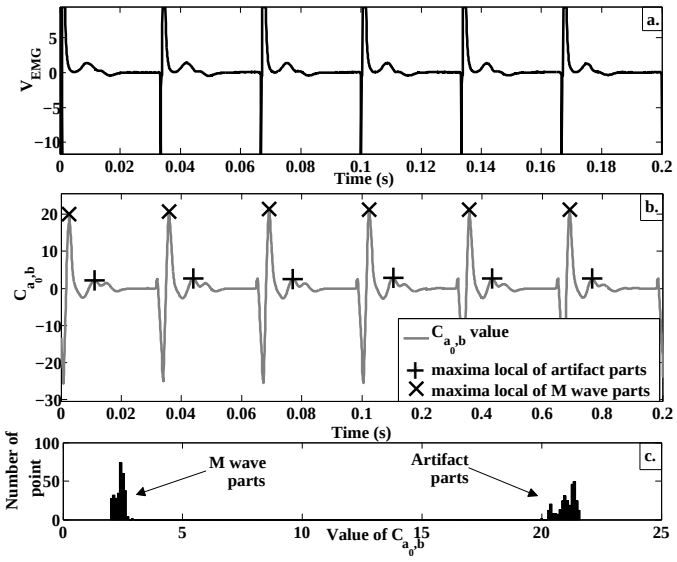

Figure 2: a) V_{EMG} signal example with an electrical stimulation at 30 Hz frequency, a 40 mA amplitude, 1 ms pulse time duration and a biphasic waveform performed on the right biceps muscle. b) CWT transformation for the V_{EMG} signal with $a_0 = 38$ corresponding to the maximum of $C_{a,b}$ coefficient. Note the difference between maxima of $C_{a_0,b}$ coefficients during artifacts (cross) and maximums $C_{a_0,b}$ coefficients during M waves (plus) which allows the differentiation between artifacts and M waves. c) Histogram of local maxima values, showing a bimodal distribution.

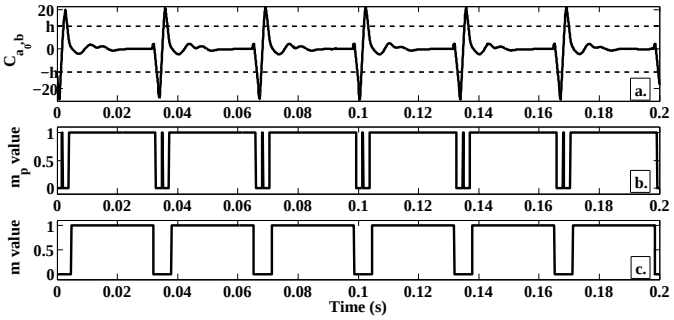

Figure 3: Creation of mask removal example. a) $C_{a_0,b}$ coefficients from CWT with a_0 scales factor. Dashed lines show h threshold representation for positive and negative parts computed with equation 2. b). Preliminary m_p mask created with h threshold. c) Final m mask from an erosion on m_p.

2.2. *Artifacts removal process*

We propose a method based on the continuous wavelet transform to detect and remove the stimulation artifacts contained in the EMG. The idea is to use a standard mother wavelet, such as the Haar wavelet, and to vary the scale factor of the continuous wavelet transform to determine which scale factor provides maximum correlation between the stimulation artifact and the wavelet coefficient. Nevertheless, the treatment should leave unchanged the M waves contained in stimulation artifacts in order to allow the extraction of physiological muscle state parameters present in M waves, such as muscular fatigue level.

In order to initialize the artifact removal process, the CWT uses the Haar wavelet. Then, tests are performed with different kinds of artifacts shapes. Next, other standard mother wavelets were applied in the CWT such as Daubechies or Symlets.

2.2.1. *Best scale factor determination*

The Haar wavelet has the characteristic to look like the stimulation artifacts in the sense that the artifact has a rectangular shape (rising and falling sharp edges), due to the amplifier saturation, as the Haar mother wavelet. This wavelet therefore might properly detect artifacts. However, the scale factor of Haar wavelet which best fit the artifact pattern has yet to be determined. To find it, the continuous wavelet transform was applied between EMG with artifacts named V_{EMG} and a wavelet ψ (Haar wavelet) undergoing a scale factor a, such that

$$C_{a,b}(V_{EMG}(t), \psi(t)) = \int_{-\infty}^{\infty} V_{EMG}(t) \frac{1}{\sqrt{a}} \psi\left(\frac{t-b}{a}\right) dt, \quad (1)$$

where b is the temporal localization. Scale factors were investigated from 1 to 100 with a step interval of 1. This range allowed the analysis of different artifact durations. Figure 1 illustrates the continuous wavelet transform, named $C_{a,b}$, with the above parameters. The V_{EMG} signal used to perform this example corresponds to that shown in Figure 2a. In order to find which scale factor a corresponds to the maximum of correlation with artifacts of V_{EMG}, we estimated the scale factor which corresponded to the maximal value of the CWT coefficients. In Figure 1, an example of $C_{a,b}$ is plotted where the value of scale factor name a_0 is obtained such that the maximum value of the $C_{a,b}$ matrix best matches the artifacts.

2.2.2. *Mask removal determination*

Once the scale factor a_0 has been found, we determine a temporal mask, allowing the removal of artifacts, with the CWT coefficients $C_{a,b}$ which correspond with this scale factor a_0 (providing the coefficient vector $C_{a_0,b}$). In the Figure 2b, an example of a continuous wavelet transform is shown on a V_{EMG} signal recorded with an electrical stimulation at a 30 Hz frequency, a 40 mA amplitude, 1 ms pulse time duration and a biphasic waveform. Only the 0.2 first second of the 6 seconds stimulation are displayed for a better readability. In this instance, the a_0 scale factor found was 38. The curve in the panel b corresponds to the continuous wavelet transform $C_{a,b}$ cross section, from the figure 1, with a scale factor $a = a_0$. It is interesting to see that the values of $C_{a_0,b}$ corresponding to artifacts are larger than the values $C_{a_0,b}$ corresponding to M waves. Thanks to this point, it is possible to distinguish both artifact and M wave parts. A threshold is created with a local maxima algorithm which is used to find maxima coefficients during stimulation artifacts and maxima coefficients during M waves. In the Figure 2b, a representation of this detection is shown with cross symbol (during artifacts) and plus symbol (during M waves). In the Figure 2c, the histogram of these points is plotted revealing a bimodal distribution. The threshold which allows identification of stimulation artifacts without disturbing M waves is located between these two distributions. We use the centroid of the points in the histogram representation as our threshold because it efficiently separates both distributions. The centroid is computed as:

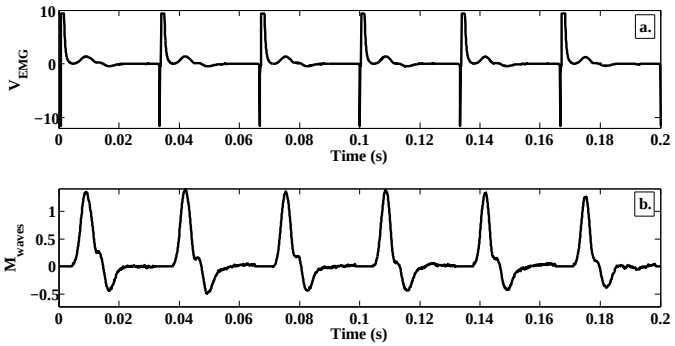

Figure 4: a) V_{EMG} signal example with an electrical stimulation at a 30 Hz frequency, a 40 mA amplitude, 1 ms pulse time duration and a biphasic waveform performed on the right biceps muscle. b) M_{waves} result example with m mask in the Figure 3c applied on the above V_{EMG} signal, note the visually acceptable removal of artifact parts.

$$h = \frac{\sum_{i=1}^{n} x_i y_i}{\sum_{i=1}^{n} y_i}, \tag{2}$$

where h is the centroid value, x_i are abscissa of the histogram, y_i are ordinate of the histogram and n is the number of the histogram range. Then, when the threshold is computed, a mask removal is created by using $|C_{a_0,b}|$ absolute coefficient values and the h threshold. The mask is equal to 1 if $|C_{a_0,b}|$ are below the threshold, which corresponds to the M wave parts. The mask is equal to 0 if $|C_{a_0,b}|$ are above the threshold, corresponding to the stimulation artifact parts. Therefore,

$$m_p = \begin{cases} 1 & \text{if } |C_{a_0,b}| < h, \\ 0 & \text{if } |C_{a_0,b}| \geq h, \end{cases} \tag{3}$$

where m_p is the preliminary mask which needs to be corrected. Indeed, in Figure 3, an example of mask removal creation is shown. The $C_{a_0,b}$ coefficient values are plotted in Figure 3a and the threshold is represented with the dash lines. Note that during the stimulation artifacts (see Fig. 3b), the preliminary mask m_p changes states. To correct that, an erosion algorithm (a mathematical morphology operation [27]) is applied to the preliminary mask vector and gives the final mask named m. An example of the corrected mask after the erosion process is shown in the Figure 3c.

2.2.3. *Stimulation artifacts removal*

The last step of artifact removal consists of multiplying the m mask, created previously, by V_{EMG} to obtain the EMG signal without stimulation artifacts named M_{waves}.

$$M_{waves}(t) = V_{EMG}(t) \cdot m(t), \tag{4}$$

The aim of the next section is to apply the artifact removal process, presented here, with different kinds of electrical stimulation because modifications of the stimulation induce changes of artifact and M wave shapes in the EMG signal [28].

3. Results

The previous section introduced the method of stimulation artifact removal using the CWT. An example of M_{waves} is shown in the Figure 4b which corresponds to the stimulation artifact removal performed on the V_{EMG} signal with an electrical stimulation at a 30 Hz frequency, a 40 mA amplitude, 1 ms pulse time duration and a biphasic waveform, represented in Figure 4a. As we can see, artifacts are removed from V_{EMG}, only M wave parts are preserved. The CWT with a Haar mother wavelet is therefore a suitable method to remove stimulation artifacts. However, as the method used is based on thresholding even in wavelet domain, the parts where artifact and M wave are merged cannot be correctly distinguished.

We used, previously, an example with a V_{EMG} signal where artifacts were higher than M waves but that is not always the case. In order to check the artifact removal process for this particular instance, the V_{EMG} signal has been truncated in amplitude during artifacts parts to make both artifacts and M waves amplitudes approximately equivalent. The V_{EMG} signal is then limited to the maximum and minimum values of all contained M waves in the signal. An example is shown in the Figure 5a. In this condition, thresholding techniques which are applied on V_{EMG} signal itself [16] are not suitable because, whatever the threshold value is, it belongs to both artifacts and M waves. Therefore, to use a thresholding technique, the V_{EMG} signal must be transformed. Our algorithm performs this transformation using the CWT whose coefficients are shown in the Figure 5b. We see that, even if both artifacts and M waves are in the same range of magnitude, the CWT coefficients results are not. The $C_{a_0,b}$ during artifacts are higher than during M waves which allow thresholding techniques. Thanks to the histogram representation, plotted in the Figure 5c, the h threshold is found with centroid determination ($h = 7.3$) and used to perform the stimulation artifact removal. The result of this example is shown in the Figure 5d and we see that artifacts are removed from the V_{EMG} signal (Fig 5a).

In section 2.2, we saw an example of CWT based stimulation artifact removal for a biphasic pulse shape. That kind of shape is common but it is not the only one, therefore, we tested two other kinds in order to check if the algorithm is suitable for monophasic and dual biphasic stimulation pulse shapes. In Figure 6, we show these two examples. One corresponds to a monophasic pulse shape and is presented in panels a, b, c and d. The other one is for a dual biphasic pulse shape which corresponds to panels e, f, g and h. Both stimulations share parameters which include a 50 Hz frequency, a 50 mA amplitude and 1 ms pulse time duration. We see that the waveforms during the artifacts change according to the shape of the stimulation pulse, when compared to the biphasic case (see Fig. 6a, e and Fig. 2a). However, the CWT transform $C_{a_0,b}$ (see Fig. 6b, f and Fig. 2b) does not seem affected by those artifact shape modifications, therefore, it is still possible to distinguish artifact and M wave parts thanks to the histogram representation (see Fig. 6c and g). After the h threshold and m mask determination, the artifact removal results give the M_{waves} signal in the Figure 6d and h.

The shape of artifacts also evolves if the duration of stimulation pulse changes. In order to check the sensibility of this modification on the artifact removal algorithm, three durations of a biphasic pulse shape have been applied. Figure 7 shows

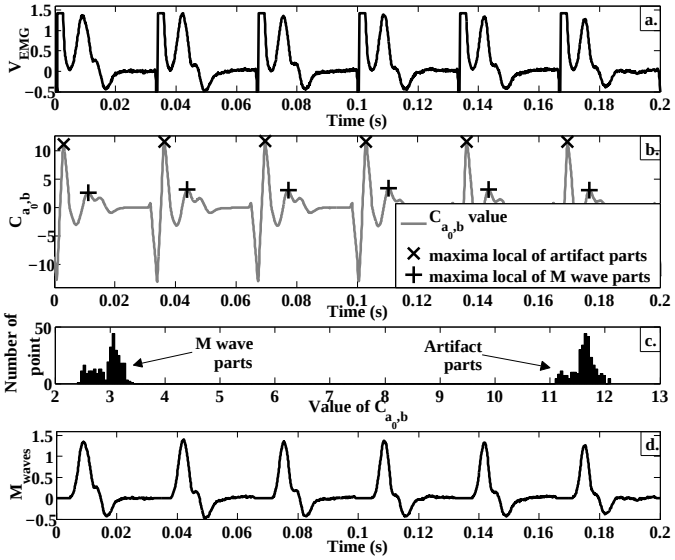

Figure 5: a) Examples of V_{EMG} signal where the artifacts magnitudes are in the same order than the M waves magnitudes. b) CWT coefficients corresponding to the best scale factor a_0. the crosses and plus represent the local maxima of $C_{a_0,b}$ coefficients respectively during artifacts and during M waves. c) Histogram of local maxima values. We discern a bimodal distribution. d) Result of artifacts removal.

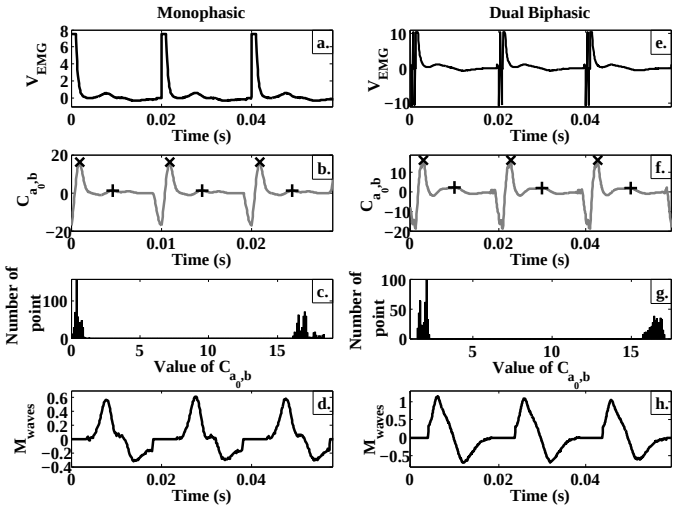

Figure 6: Examples for different stimulation pulse shapes. a monophasic pulse shape which corresponds to panels from a to d and a dual biphasic pulse shape which corresponds to panels from e to h. Both stimulations share the following parameters: a 50 Hz frequency, a 50 mA amplitude and 1 ms pulse time duration. a & e) Examples of V_{EMG} signal where the pulse stimulation is monophasic and dual biphasic. b & f) CWT coefficients corresponding to the best scale factor a_0. The cross and plus symbols represent the local maxima of $C_{a_0,b}$ coefficients during artifacts and during M waves. c & g) Histograms of local maxima values showing a bimodal distribution. d & h) Results of artifacts removal.

examples for 1 ms, 1.5 ms and a 2 ms pulse durations. We see a modification of V_{EMG} signal during the artifacts (Fig 7a, e and i). The longer the stimulation pulses are, the longer the artifacts are. Therefore, the removal process must detect this time length variation. Figures 7b, f and j show that the wavelet domain still leads to the distinction of both artifact and M wave parts thanks to the bimodal distribution, on the histogram representation in the Figures 7c, g and k. We see, in Figures 7d, h and i, the resulting M_{waves} signals showing that, even if the duration of artifacts evolves, the process is able to completely remove artifact parts.

The CWT based technique proposed here removes stimulation artifacts in an EMG signal. It gives visually acceptable results for different kinds of stimulation pulse shapes and pulse durations even if the amplitude of artifacts and M waves are in the same range of values which cannot be performed with thresholding method directly applied on V_{EMG} signal. We used previously the Haar mother wavelet to perform CWT, in order to introduce this method, but it is possible to use other common mother wavelets. In Figure 8, we show the use of other mother wavelets which are widely used in CWT treatments. Mother wavelets used included: Daubechies, Symlets, Gaussian, Coiflet, Morlet, Meyer and Shannon wavelets. We see that the majority of mother wavelets gives reasonable results with a good visual removal of stimulation artifacts. However, some are less efficient than others. Cases in point "Sym3" and "shan1-1" which do not completely remove artifacts. If parts of artifact remain in the M_{waves} signal, they could lead to estimation error during successive signal processing techniques to determine physiological characteristics contained in EMG signal such as muscular fatigue level. This is the case for "morl" and "meyr". Here, artifact parts are completely removed but the trouble is that the M wave parts are truncated, potentially leading to M wave parameter estimation errors in subsequent processing. With the purpose to find the wavelet which best handle both artifact and M wave parts, we investigate an index to classify wavelets. For each kind of wavelet, this index characterizes the distance between the two distributions in the histogram representation performed from the local maxima of $C_{a_0,b}$ during artifacts and M waves (see the Figure 2c). If this distance is large, the h threshold easily shares artifact and M wave parts. However, if this distance is too small, the h threshold could not distinguish between artifact and M wave parts, which can create problems as Figure 8 shows with "sym3" or "morl". The distance between the two distributions is computed by using the centroid of each distribution. With regard to the histogram in the Figure 2c for instance, a centroid c_l is computed by using the lowest values of the histogram. Therefore, c_l gives information about the position of local maxima during M wave parts. In the same way, a centroid c_h is computed by using the highest values of the histogram which correspond to local maxima during artifacts. The centroids c_l and c_h are calculated such that:

$$c_l = \frac{\sum_{i=1}^{p} xl_i yl_i}{\sum_{i=1}^{p} yl_i}, \tag{5}$$

where p is the number of points, xl_i is the abscissa and yl_i is the ordinate according to the lowest values of the histogram;

$$c_h = \frac{\sum_{i=1}^{q} xh_i yh_i}{\sum_{i=1}^{q} yh_i}, \tag{6}$$

where q is the number of points, xh_i is the abscissa and yh_i is the

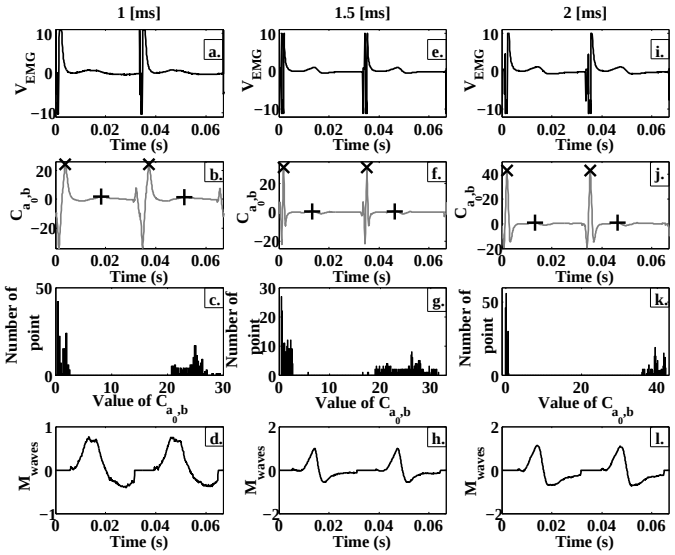

Figure 7: Examples for three different stimulation pulse durations, 1 ms (from a to d), 1.5 ms (from e to h) and a 2 ms (from i to l). All stimulations share the following parameters: a 30 Hz frequency, a 50 mA amplitude and a biphasic shape. a, e & i) Example of V_{EMG} signal where the pulse duration are 1, 1.5 and 2 ms long. b, f & j) CWT coefficients corresponding to the best scale factor a_0. the cross and plus symbols represent the local maxima of $C_{a_0,b}$ coefficients respectively during artifacts and during M waves. c, g & k) Histogram of local maxima values showing a bimodal distribution. d, h & l) Result of artifacts removal.

ordinate according to the highest values of the histogram. The number of artifacts is equal to the number of M wave, therefore $p = q$. The distance between the two distributions Δ_c is computed as the difference between the two centroids c_l and c_h such that

$$\Delta_c = c_h - c_l. \tag{7}$$

In order to find the mother wavelet which best separated the artifacts and M waves in the wavelet domain, we computed Δ_c for several V_{EMG} signals with different stimulation parameters (amplitude, frequency, pulse duration and pulse waveform) and different subjects for a total dataset of fifty samples. For each V_{EMG} signal, Δ_c was computed for the fourteen mother wavelets (noted $k \in \mathbb{N} = [1 : 14]$) presented in the Figure 8 and have been normalized with respect to the highest Δ_{c_k} among the fourteen (so, one $max(\Delta_c)$ per V_{EMG} signal), as

$$\Delta'_{c_k} = \frac{\Delta_{c_k}}{max(\Delta_c)}. \tag{8}$$

Then, the median of each Δ'_{c_k} was calculated establishing an index for determining which wavelet most efficiently removed artifacts. The closer to 1 the index, the better artifacts and M waves were distinguished. Figure 9 shows the results of Δ'_c for each wavelet referenced in Figure 8. We observed that the mother wavelet with poor artifact removal corresponded to a low median index value. This was the case for "shan", "sym2" and "sym3", which lacked complete artifact removal, and "morl" and "meyr", which truncated M waves. The mother wavelet which provided the highest index was the Haar wavelet. In addition, the gaus1 mother wavelet seams to be a suitable

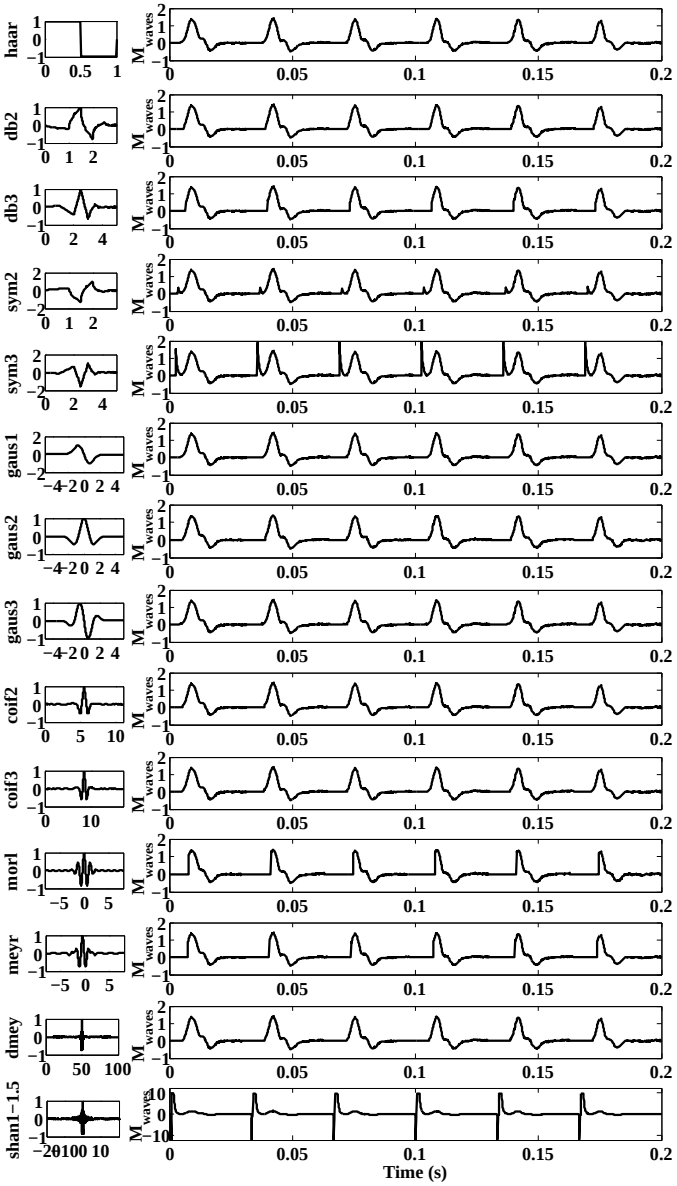

Figure 8: Examples of artifacts removal with Haar wavelet (haar), Daubechies wavelets (db2 and db3), Symlets wavelets (sym2 and sym3), Gaussian wavelets (gaus1, gaus2 and gaus3), Coiflet wavelet (coif2 and coif3) , Morlet wavelet (morl), Meyer wavelet (meyr, dmey) and Shannon wavelet (shan1-1) applied on the V_{EMG} signal from Figure 2a.

candidate. Nevertheless, note that the use of the Haar wavelet gives statistically slightly better results, when considering also the 25th and 75th percentiles and the minimum and maximum values for Δ'_c.

However the distance between each distribution is not the only factor that can be analyzed to show the ability of a mother wavelet to split efficiently artifact and M wave parts. We also studied the variance of distributions. If the distance between each distribution is large and the variances are high, then a part of each distribution could be merged to each other making the differentiation difficult. Therefore, in order to find the best mother wavelet, a Gaussian curve g is found for each distribution with two parameters: the mean (c_z) and the variance

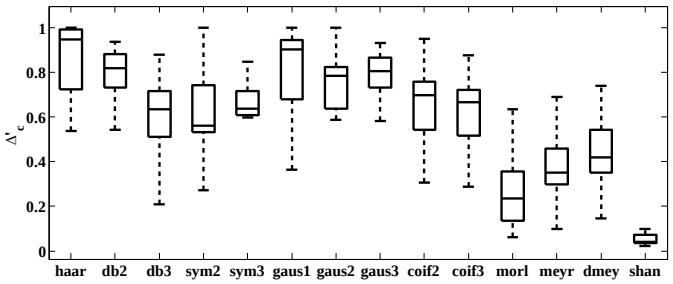

Figure 9: Δ'_c index computed for each mother wavelet from Figure 8 according to equation 8. The Haar mother wavelet provided the highest index value and best distinguished artifacts in V_{EMG} signals.

values (σ_z^2) of the histogram. Gaussian curves were computed such that,

$$g_z(C) = \frac{1}{\sigma_z \sqrt{2\pi}} e^{-\frac{1}{2}\left(\frac{C-c_z}{\sigma_z}\right)^2}, \tag{9}$$

where z is either l for the lowest values of the histogram (corresponding to M waves) or h for the highest values of the histogram (corresponding to artifacts). Then, after g_l and g_h is determined, the area A which is common to both Gaussians is computed so that,

$$A = \int_{-\infty}^{\infty} min\left[g_l(C), g_h(C)\right] dC. \tag{10}$$

In this way, as the area of each Gaussian is 1, if the common area of both Gaussian is close to 1 then the two histograms are merged and if A is close to zero then the two histograms are well split. In this last case, the wavelet is well able to separate artifact and M wave parts. The Figure 10 a to c show three examples with panel 10a illustrating a suitable use of mother wavelet and panel 10c a use of an unsuitable mother wavelet. In the Figure 10d, the result of the area calculation (A) is shown for several V_{EMG} signals with different stimulation parameters (amplitude, frequency, pulse duration and pulse waveform) and different subjects for a total dataset of fifty samples. The results of each wavelet have been computed and represented in a boxplot. We observed that the mother wavelets which poorly removed artifacts provided higher median area values and a higher variability. This is the case for "shan", "sym2" and "sym3", which cannot remove entirely artifacts, and also "morl" and "meyr", which truncate M waves. The mother wavelet which displayed the lowest median index and the smallest variability was the Haar wavelet. Mother wavelets gauss1 and gauss2 are also good candidates. The common area index A could be used in hybrid system where the proposed method could be applied on a signal if this index is sufficiently low. If it is not, another method could be used. However, to obtain this index, the wavelet transform computation is needed and could cost a non negligible execution time on hybrid process.

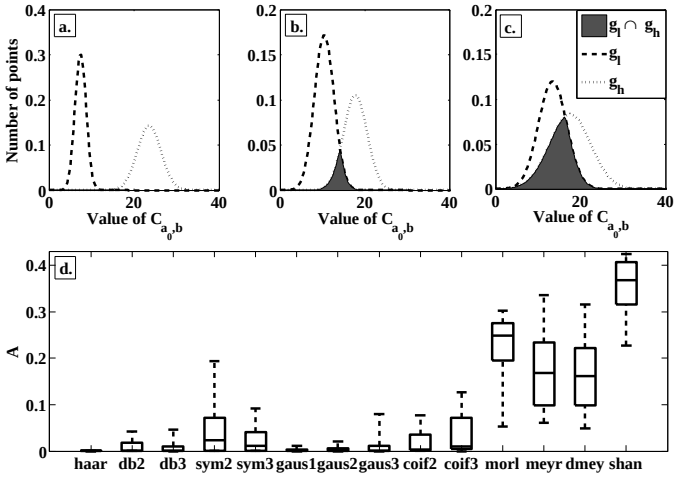

Figure 10: a to c) plots of the two Gaussians g_l and g_h and their intersection. a shows an example where both Gaussian are well split, so the corresponding mother wavelet allows a suitable artifacts detection. In b, Gaussians start to be merged and, in c, Gaussians are almost completely merged so the corresponding wavelet does not allow a suitable detection of artifacts. d) Mean area A computed for each mother wavelet according to the equation 10. The Haar mother wavelet displayed the lowest value. Therefore, it is the most able to remove artifacts from V_{EMG} signals.

4. CONCLUSION

In this study, a new stimulation artifact removal algorithm for EMG signal recorded during electrically evoked contraction is presented. The technique is based on continuous wavelet transform to convert the EMG signal into the wavelet domain and a histogram representation, which gives a bimodal distribution. It leads to the distinguishment of artifacts from M wave parts on an EMG signal recorded during an electrical muscle stimulation. Such that, once the artifact parts are found, the treatment can suppress them. Some examples are given and show the algorithm ability to detect artifacts and remove them in different circumstances especially when the shape and the duration of electrical stimulation pulses are modified, which leads to a modification of artifact waveform. We included tests with changes in amplitude, pulse train frequency, pulse duration and pulse shape. When artifacts and M waves are in the same range of amplitude, the wavelet based technique is also able to remove artifacts. We performed tests for many mother wavelets with visually acceptable results except for "Sym3", "shan1-1", "gaus3" and "meyr" which allowed passage of artifact parts or truncated M wave parts. In order to determine which mother wavelet gives the best results, two indexes have been created. One uses the distance between the centers of the two distributions in the histogram representation. The other uses, in addition, the variance thanks to a Gaussian fitting of the histogram where the common area among the two Gaussian is the index. If this area is high then the wavelet is not adapted to distinguish artifacts in EMG signal. Those two indexes determined that the Haar wavelet is the most suitable to distinguish both artifact and M wave parts because the distance between both centroid is the highest and the common area of Gaussians is the smallest. In this work, we used standard mother wavelets, however, instead of using standard mother wavelets, it could be possible to create a new mother wavelet from an artifact signal itself. In this way, the artifact removal could be adapted for any kind of stimulation pulses or subjects. That could make the treatment

more efficient. This stimulation artifact removal can be used as a signal pre-processing step with an EMG signal recording over an electrical stimulation evoked contraction. A possible next study will be to compare this wavelet approach for artifact removal with other ones already used in the literature. For instance, filtering methods can attenuate artifact when they are merged with M wave which is not possible with a thresholding technique as the method proposed here. Another work could be to optimize the execution time which could be a limitation for real time applications due to the wavelet domain conversion.

References

[1] A. E. Hines, P. E. Crago, G. J. Chapman, C. Billian, Stimulus artifact removal in emg from muscles adjacent to stimulated muscles, Journal of neuroscience methods 64 (1) (1996) 55–62.

[2] P. Konrad, The abc of emg, A practical introduction to kinesiological electromyography 1,(2005).

[3] M. Zwarts, G. Drost, D. Stegeman, Recent progress in the diagnostic use of surface emg for neurological diseases, Journal of Electromyography and Kinesiology 10 (5) (2000) 287–291.

[4] F. Mandrile, D. Farina, M. Pozzo, R. Merletti, Stimulation artifact in surface emg signal: effect of the stimulation waveform, detection system, and current amplitude using hybrid stimulation technique, Neural Systems and Rehabilitation Engineering, IEEE Transactions on 11 (4) (2003) 407–415.

[5] M. Knaflitz, R. Merletti, Suppression of stimulation artifacts from myoelectric-evoked potential recordings, Biomedical Engineering, IEEE Transactions on 35 (9) (1988) 758–763.

[6] M. Reaz, M. Hussain, F. Mohd-Yasin, Techniques of emg signal analysis: detection, processing, classification and applications, Biological procedures online 8 (1) (2006) 11–35.

[7] M. Solomonow, R. Baratta, T. Miwa, H. Shoji, R. D'Ambrosia, A technique for recording the emg of electrically stimulated skeletal muscle., Orthopedics 8 (4) (1985) 492.

[8] T. Wichmann, A digital averaging method for removal of stimulus artifacts in neurophysiologic experiments, Journal of neuroscience methods 98 (1) (2000) 57–62.

[9] E. Roskar, A. Roskar, Microcomputer based electromyographic recording system with stimulus artifact suppression, in: Third Medical Conference on Biomedical Engineering, Portoroz Yugoslavia, 1983.

[10] R. Roby, E. Lettich, A simplified circuit for stimulus artifact suppression, Electroencephalography and Clinical Neurophysiology 39 (1) (1975) 85–87.

[11] J. Freeman, An electronic stimulus artifact suppressor, Electroencephalography and clinical neurophysiology 31 (2) (1971) 170–172.

[12] T. L. Babb, E. Mariani, G. M. Strain, J. P. Lieb, H. V. Soper, P. H. Crandall, A sample and hold amplifier system for stimulus artifact suppression, Electroencephalography and clinical neurophysiology 44 (4) (1978) 528–531.

[13] Z. M. Nikolic, D. B. Popovic, R. B. Stein, Z. Kenwell, Instrumentation for eng and emg recordings in fes systems, Biomedical Engineering, IEEE Transactions on 41 (7) (1994) 703–706.

[14] K. McGill, K. Cummins, L. Dorfman, B. Berlizot, K. Luetkemeyer, D. Nishimura, B. Widrow, On the nature and elimination of stimulus artifact in nerve signals evoked and recorded using surface electrodes, Biomedical Engineering, IEEE Transactions on (2) (1982) 129–137.

[15] Z. Lin, R. W. McCallum, Adaptive stimulus artifact cancellation in gastric myoelectrical signals, in: Engineering in Medicine and Biology Society, 1998. Proceedings of the 20th Annual International Conference of the IEEE, Vol. 3, IEEE, 1998, pp. 1636–1639.

[16] D. O'Keeffe, G. Lyons, A. Donnelly, C. Byrne, Stimulus artifact removal using a software-based two-stage peak detection algorithm, Journal of neuroscience methods 109 (2) (2001) 137–145.

[17] G. Harding, A method for eliminating the stimulus artifact from digital recordings of the direct cortical response, Computers and biomedical research 24 (2) (1991) 183–195.

[18] D. A. Wagenaar, S. M. Potter, Real-time multi-channel stimulus artifact suppression by local curve fitting, Journal of neuroscience methods 120 (2) (2002) 113–120.

[19] R. I. Barbosa-Mier, A. Carrillo Chica, J. Vega Riveros, Comparison of adaptive systems for suppression of stimulation artifacts in emg signals, in: Devices, Circuits and Systems, 1995., Proceedings of the 1995 First IEEE International Caracas Conference on, IEEE, 1995, pp. 144–148.

[20] K. S. Türker, Electromyography: some methodological problems and issues, Physical Therapy 73 (10) (1993) 698–710.

[21] J. Rafiee, M. Rafiee, N. Prause, M. Schoen, Wavelet basis functions in biomedical signal processing, Expert Systems with Applications 38 (5) (2011) 6190–6201.

[22] D. Farina, A. Blanchietti, M. Pozzo, R. Merletti, M-wave properties during progressive motor unit activation by transcutaneous stimulation, Journal of Applied Physiology 97 (2) (2004) 545–555.

[23] M. Yochum, T. Bakir, R. Lepers, S. Binczak, A real time electromyostimulator linked with emg analysis device, IRBM 34 (1) (2013) 43–47.

[24] M. Yochum, T. Bakir, R. Lepers, S. Binczak, Estimation of muscular fatigue under electromyostimulation using cwt, IEEE transaction on Biomedical Engineering 59 (12) (2012) 3372–3378.

[25] Biodex, http://www.biodex.com/physical-medicine/products/dynamometers, biodex system 3 pro (2014).

[26] R. Merletti, D. Farina, Surface emg processing: Introduction to the special issue, Biomedical Signal Processing and Control 3 (2) (2008) 115–117.

[27] J. Serra, Image analysis and mathematical morphology, 1982.

[28] R. Merletti, M. Knaflitz, C. J. De Luca, et al., Electrically evoked myoelectric signals, Crit Rev Biomed Eng 19 (4) (1992) 293–340.